Wave-packet solution to the time-dependent arrangement-channel quantum-mechanics equations

Z. H. Zhang and D. J. Kouri
Department of Physics and Department of Chemistry, University of Houston, University Park, Houston, Texas 77004
(Received 25 November 1985)

The time-dependent arrangement-channel quantum-mechanics (ACQM) equations are numerically solved for the collinear exchange reaction $H+H_2$. The method employs the fast-Fourier-transform scheme of Kosloff and Kosloff and an efficient time propagator involving a Chebyshev polynomial expansion due to Tal-Ezer and Kosloff. The time-dependent ACQM formalism, which is based on the use of the time-dependent arrangement-channel-component states as introduced by Kouri, Kruger, and Levin, involves a non-Hermitian matrix Hamiltonian in arrangement-channel space. We employ the channel-permuting array-coupling sequence of Baer, Kouri, Levin, and Tobocman. The remarkable property of the channel-component states that, below the dissociation threshold, only the component in channel j gives rise to outgoing waves in that arrangement channel, is explicitly seen in this time-dependent calculation. The calculated reaction probability is in reasonable agreement with the time-independent calculation result. The question of whether the numerically generated time-dependent solutions contain spurious solutions (which can arise in principle, due to the matrix nature of the Hamiltonian in arrangement-channel space) is discussed. It is found computationally that such spurious solutions do not create any difficulties in the calculation of reactive probabilities within the time-dependent ACQM formalism.

I. INTRODUCTION

Reactive scattering theory mainly has been studied by time-independent calculation methods. There are two basic approaches for chemical systems. The most widely used and familiar is the differential equation approach,[1] which basically propagates the wave function within the various possible arrangements and matches it on certain surfaces separating different arrangement channels. If one uses some type of reaction coordinate,[2] the integro-differential equation approach,[3] or the finite-element method,[4] then the matching step can be avoided. The second general approach is to solve the coupled integral equations for the various possible arrangement scattering amplitudes directly.[5] The integral equations explicitly incorporate all possible boundary conditions, and therefore no matching is encountered. The so-called Baer-Kouri-Levin-Tobocman[6] (BKLT) equations have been successfully applied numerically to collinear reactive scattering problems with smooth potential surfaces recently[7] and extension to full three-dimensional problems is currently under way. The general time-dependent formalism of arrangement-channel quantum-mechanics (ACQM) equations[8] has not yet been numerically applied to reactive scattering. Chemical reactions are time-dependent phenomena, so an interesting way of dealing with them is to use time-dependent quantum mechanics. There are computational difficulties associated with the time-dependent approach to dynamics which so far have inhibited the use of time-dependent QM as a general tool in chemical reaction studies. On the other hand, the time-dependent method has the virtue that it gives direct insight to the solution, i.e., the results are easy to interpret, it is in principle a powerful tool for studying intimate details of the collision processes (such as perhaps the time delay[9] to distinguish whether the reaction is direct or complex). The time-dependent method can also be used to study collision-induced dissociation (CID) (Ref. 10) where the standard close-coupling method is very difficult because it involves a continuously infinite number of basis functions.

In this study, a wave-packet approach is used to solve the time-dependent ACQM equations for the $H+H_2$ system and reaction probabilities are compared with those obtained from other methods.[11] The arrangement-channel-component wave-function magnitudes are plotted at different time steps as well as the total physical wave-function probability densities, to demonstrate the evolution of the wave-function components as time progresses. These channel-component states satisfy the time-dependent BKLT equations (collinear)[6,8]

$$\begin{aligned} i\frac{\partial}{\partial t}\Psi_1 &= H_1\Psi_1 + V_2\Psi_2 , \\ i\frac{\partial}{\partial t}\Psi_2 &= H_2\Psi_2 + V_1\Psi_1 , \end{aligned} \tag{1}$$

with the initial condition

$$\begin{aligned} \Psi_1(t=0) &= \Phi(R)\chi_0(r) , \\ \Psi_2(t=0) &= 0 , \end{aligned} \tag{2}$$

where $\Phi(R)$ is a Gaussian wave packet and $\chi_0(r)$ is a diatomic vibrational eigenfunction in the initial arrangement.

It will be evident later that Ψ_2 remains zero until Ψ_1 moves into the interaction region. Then Ψ_2 gradually picks up strength due to the coupling with Ψ_1 in the interaction region.

II. THEORY

A. ACQM equation and mass-scaled coordinates

The general time-dependent ACQM equations resemble the ordinary Schrödinger equation except that the simple Hamiltonian is replaced by a matrix Hamiltonian operator in arrangement-channel space,

$$i\frac{\partial}{\partial t}\Psi(t)=\underline{H}\Psi(t)\ , \tag{3}$$

here

$$\Psi=\begin{bmatrix}\Psi_1\\ \Psi_2\\ \vdots\\ \Psi_{n-1}\\ \Psi_n\end{bmatrix} \tag{4}$$

and

$$\underline{H}=\begin{bmatrix}H_1 & V_2 & 0 & \cdots & & & 0\\ 0 & H_2 & V_3 & 0 & \cdots & & 0\\ \vdots & & & \ddots & & & \vdots\\ 0 & \cdots & & & 0 & H_{n-1} & V_n\\ V_1 & 0 & \cdots & & & 0 & H_n\end{bmatrix} \tag{5}$$

or more explicitly, with the BKLT coupling sequence

$$\begin{aligned}&\left[i\frac{\partial}{\partial t}-H_1\right]\Psi_1(t)=V_2\Psi_2(t)\ ,\\ &\left[i\frac{\partial}{\partial t}-H_2\right]\Psi_2(t)=V_3\Psi_3(t)\ ,\\ &\vdots\\ &\left[i\frac{\partial}{\partial t}-H_n\right]\Psi_n(t)=V_1\Psi_1(t)\ .\end{aligned} \tag{6}$$

The cyclic coupling is due to the introduction of the channel-permuting array.[6] Adding these equations together gives rise to the ordinary Schrödinger equations

$$i\frac{\partial}{\partial t}\Psi(t)=H\Psi\ , \tag{7}$$

with

$$\Psi=\sum_{i=1}^{N}\Psi_i \tag{8}$$

and

$$H=H_i+V_i\quad(i=1,2,\ldots N)\ . \tag{9}$$

We note that if $\Psi=\sum_{i=1}^{N}\Psi_i$ is nonzero, it must correspond to a solution of the time-dependent Schrödinger equation. However, it can in principle occur that the sum over the components Ψ_i vanishes everywhere. In that case we refer to the solution as a spurious solution[8] since it corresponds to a nontrivial solution of the equations for Ψ_i but to a trivial solution of the ordinary time-dependent Schrödinger equation. In a collinear exchange collision, $N=2$ and the ACQM equation is simply the following:

$$\begin{aligned}&\left[i\frac{\partial}{\partial t}-H_1\right]\Psi_1=V_2\Psi_2\ ,\\ &\left[i\frac{\partial}{\partial t}-H_2\right]\Psi_2=V_1\Psi_1\ ,\end{aligned} \tag{10}$$

or in compact form

$$i\frac{\partial}{\partial t}\Psi(t)=\underline{H}\Psi(t)\ , \tag{11}$$

where

$$\Psi=\begin{bmatrix}\Psi_1\\ \Psi_2\end{bmatrix} \tag{12}$$

and

$$\underline{H}=\begin{bmatrix}H_1 & V_2\\ V_1 & H_2\end{bmatrix}\ . \tag{13}$$

It is easy to see that

$$\underline{H}^{\dagger}=\begin{bmatrix}H_1 & V_1\\ V_2 & H_2\end{bmatrix}\neq\underline{H} \tag{14}$$

due to the off-diagonal elements in the potential matrix. This means

$$i\frac{\partial}{\partial t}\langle\Psi^T\,|\,\Psi\rangle=\langle\Psi^T\,|\,(\underline{H}-\underline{H}^{\dagger}\,|\,\Psi\rangle\neq 0\ . \tag{15}$$

It is expected that for nonorthogonal Ψ_1 and Ψ_2

$$i\frac{\partial}{\partial t}\langle\Psi^T\,|\,\Psi\rangle=\frac{\partial}{\partial t}(\langle\Psi_1\,|\,\Psi_1\rangle+\langle\Psi_2\,|\,\Psi_2\rangle)\neq 0\ . \tag{16}$$

As a matter of fact, the physical wave function is the sum of Ψ_1 and Ψ_2,

$$\Psi=\Psi_1+\Psi_2 \tag{17}$$

and the norm is

$$\langle\Psi\,|\,\Psi\rangle=\langle\Psi_1\,|\,\Psi_1\rangle+\langle\Psi_2\,|\,\Psi_2\rangle+2\,\mathrm{Re}(\langle\Psi_1\,|\,\Psi_2\rangle)\ , \tag{18}$$

which is a conserved quantity, while $\langle\Psi^T\,|\,\Psi\rangle$ is not. From (15), (16), and (18),

$$\begin{aligned}i\frac{\partial}{\partial t}\langle\Psi^T\,|\,\Psi\rangle&=i\frac{\partial}{\partial t}\langle\Psi\,|\,\Psi\rangle-2i\frac{\partial}{\partial t}\mathrm{Re}(\langle\Psi_1\,|\,\Psi_2\rangle)\\ &=-2i\frac{\partial}{\partial t}\mathrm{Re}(\langle\Psi_1\,|\,\Psi_2\rangle)\\ &=\langle\Psi^T\,|\,[\underline{H}-\underline{H}^{\dagger}]\,|\,\Psi\rangle\ .\end{aligned} \tag{19}$$

Then

$$\frac{\partial}{\partial t}\mathrm{Re}(\langle\Psi_1\,|\,\Psi_2\rangle)=-\mathrm{Im}(\langle\Psi_1\,|\,[V_2-V_1]\,|\,\Psi_2\rangle)\ . \tag{20}$$

For a more detailed discussion, see Ref. 12 (Evans and Hoffmann). The perturbation potential $V_\alpha(R_\alpha,r_\alpha)$ is defined as

$$V_\alpha = V(R_\alpha, r_\alpha) - \lim_{R_\alpha \to \infty} V(R_\alpha, r_\alpha) \tag{21}$$

and the arrangement-channel Hamiltonian H_α is

$$H_\alpha = -\frac{\hbar^2}{2u}\left[\frac{\partial^2}{\partial r_\alpha^2} + \frac{\partial_2}{\partial R_\alpha^2}\right] + V^\alpha(r_\alpha) . \tag{22}$$

Here V is the full interaction potential, and

$$V^\alpha(r_\alpha) = \lim_{R_\alpha \to \infty} V(R_\alpha, r_\alpha) \tag{23}$$

is the diatomic potential in the α arrangement channel. u is the system reduced mass,[13]

$$u = \left[\frac{m_1 m_2 m_3}{m_1 + m_2 + m_3}\right]^{1/2} . \tag{24}$$

R_α, r_α are the mass-scaled coordinates

$$R_\alpha = \lambda_\alpha \bar{R}_\alpha, \quad r_\alpha = \bar{r}_\alpha / \lambda_\alpha , \tag{25}$$

where $\bar{R}_\alpha$ and $\bar{r}_\alpha$ are the true distances (not mass scaled), and

$$\lambda_\alpha = \left[\frac{m_\beta m_\gamma (m_1 + m_2 + m_3)}{m_\alpha (m_\beta + m_\gamma)^2}\right]^{1/2}, \quad \alpha \neq \beta \neq \gamma \neq \alpha . \tag{26}$$

Then the transformation between different arrangement-channel coordinates becomes orthogonal,

$$\begin{aligned} R_\beta &= R_\alpha \cos\chi + r_\alpha \sin\chi , \\ r_\beta &= R_\alpha \sin\chi - r_\alpha \cos\chi , \end{aligned} \tag{27}$$

where χ is the skewing angle defined by

$$\tan\chi = \frac{m_\gamma}{u} . \tag{28}$$

From Eq. (17) we have the formal solution

$$\Psi(t) = \exp(-i\underline{H}t)\Psi(t=0) . \tag{29}$$

Since the eigenstates of $\underline{H}$ form a complete set,[12] we can formally expand the $\Psi(t=0)$ as

$$\Psi(t=0) = \sum_n A_n \Psi_n , \tag{30}$$

where

$$\underline{H}\Psi_n = E_n \Psi_n \tag{31}$$

so

$$\Psi(t) = \exp(-i\underline{H}t)\Psi(0) = \sum_n A_n \exp(-iE_n t)\Psi_n . \tag{32}$$

Thus $\exp(-i\underline{H}t)$ is a simple phase factor when acting on an eigenstate Ψ_n.

There are several alternatives[10,11,14–16] for evaluating the action of the time propagator $\exp[-i(\underline{H}t/\hbar)]$ on the wave packet. in general there are two aspects of concern. First is the treatment of the exponential itself either as a power series (Taylor series) or in the present instance, a series of Chebyshev polynomials of matrices. Generally, a simple Taylor expansion of the exponential does not preserve the time-reversal symmetry[16] and the truncated power series is not exactly unitary. In addition, to improve the accuracy of such an approach, it is generally necessary to use very small time steps [this is equivalent to expanding $\exp(-it\underline{H}/N\hbar)$, where N is very large so that $\Delta t \equiv t/N$ is small, and then raising the result to the Nth power]. Alternatively, one may use the Padé, approximation (e.g., see Kulander's work[10]). This is unitary, accurate to second order in Δt, and is numerically stable. However, the propagation typically takes a large number of steps and the propagator requires computation of the inverse operator $(1 + i\underline{H}\Delta t/2\hbar)^{-1}$. Accurate results require use of a relatively small Δt. The Chebyshev polynomial expansion[14,16] has the following attractive features.

(a) The error decreases exponentially once enough terms in the expansion are taken (due to the uniform distribution of the error over the domain of definition of the polynomials).

(b) The step size in the method can be made as large as desired so long as sufficient numbers of terms are included (in fact, the calculations were all done with a single time step).

(c) The propagation is stable and numerically easy to apply and does not involve any matrix inversions.

(d) The method is unitary as discussed by Kosloff and Kosloff.[14]

The second feature of the approach we employ concerns the use of the fast-Fourier-transform (FFT) method of evaluating the action of the Hamiltonian on the wave packet.[14,16] Other approaches have utilized finite difference methods for evaluating the second derivatives due to kinetic energy operators in the Hamiltonian. The FFT method[14,16] allows a reduction in the number of spatial grid points and reduces spurious numerical dispersion.

B. Chebyshev method and fast-Fourier transform

Denote the eigenvalues of $\underline{H}$ by E_n, and the minimum and maximum by $E_{\min}$ and $E_{\max}$. Then rewrite the propagator as follows:

$$\exp(-i\underline{H}t) = \exp[-i(E_{\max} + E_{\min})t/2]\exp(iR\underline{X}) , \tag{33}$$

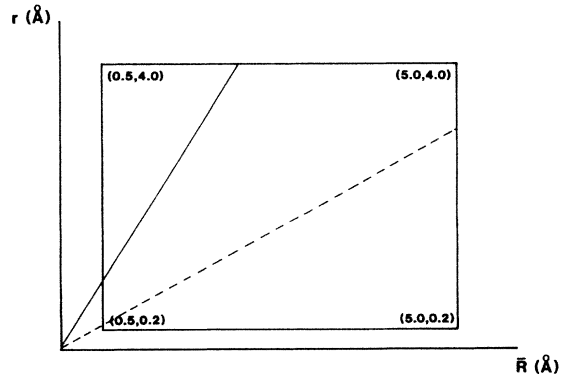

FIG. 1. Skewing angle $\chi = 60°$. The dotted line is the symmetric stretch line.

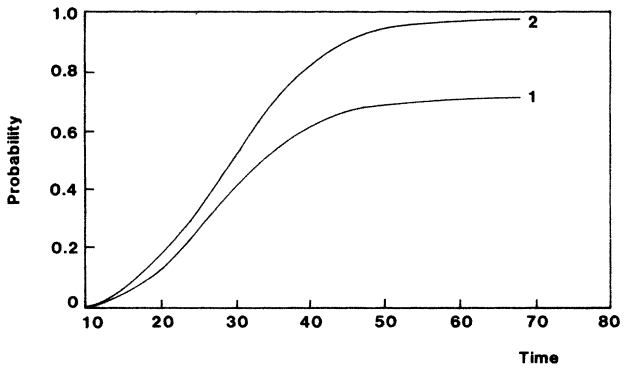

FIG. 2. Reaction probability vs time (unit of time is 6.5783×10^{-16} sec). Curve 1 is for $E_t=0.38$ eV, $\delta=0.15$ Å, $R_i=3.0$ Å; curve 2 has $E_t=0.38$ eV, $\delta=0.5$ Å, $R_i=3.0$ Å.

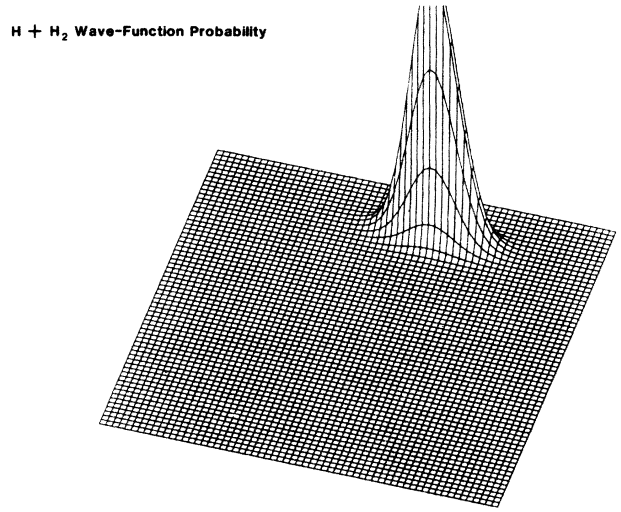

FIG. 3. ACQM component $|\Psi_1|^2$ and the full $|\Psi|^2$ at time $t=10$. Packet parameters are $E_t=0.38$ eV, $\delta=0.15$ Å, $R_i=3.0$ Å (not mass scaled). $|\Psi_2|^2$ is zero at this time.

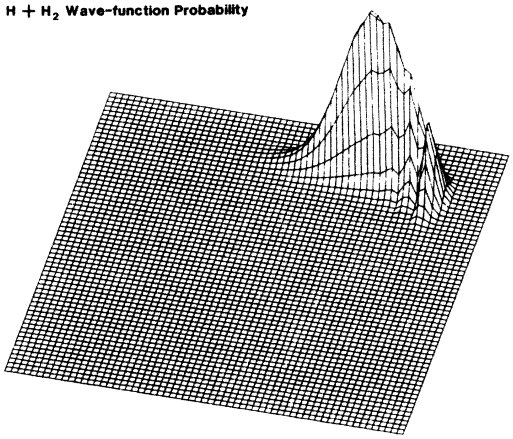

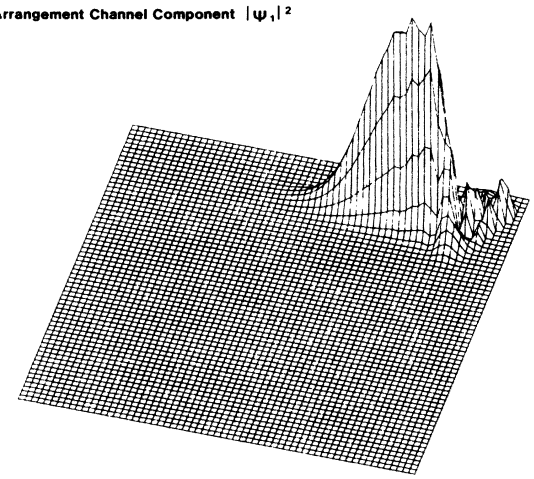

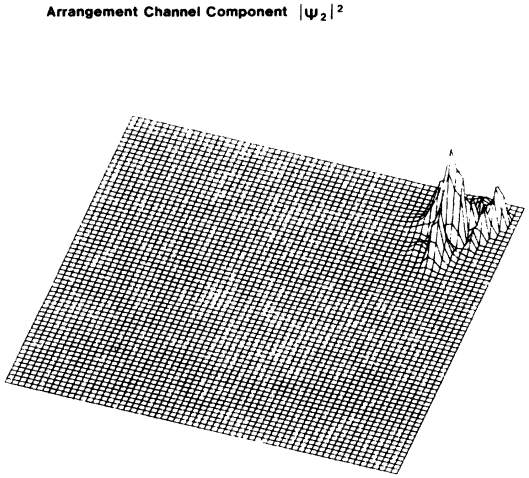

FIG. 4. ACQM components $|\Psi_1|^2$, $|\Psi_2|^2$, and the full $|\Psi|^2$ at time $t=20$.

where

$$R=(E_{\max}-E_{\min})/2 \tag{34}$$

and

$$\underline{X}=(E_{\max}+E_{\min}-2\underline{H})/(E_{\max}-E_{\min}) . \tag{35}$$

It is easy to see the eigenvalue X_n of $\underline{X}$ is within the range

$$X_n\in[-1,1] . \tag{36}$$

The first factor $\exp[-i(E_{\max}+E_{\min})t/2]$ involves no operator during the entire time propagation. Now, expand $\exp(iR\underline{X})$ in Chebyshev polynomials

$$\exp(iR\underline{X})=\sum_n A_n T_n(\underline{X}) . \tag{37}$$

Here

$$A_n=(2-\delta_{n0})i^n J_n(R) , \tag{38}$$

where $J_n(R)$ is the Bessel function of the first kind of order n.

Chebyshev polynomials satisfy the recurrence relation[17]

$$T_n(X)=2XT_n(X)-T_{n-2}(X) \tag{39}$$

and

$$T_0(X)=1, \quad T_1(X)=X . \tag{40}$$

The operation of the kinetic operator on $\underline{\Psi}$ is done symbolically as follows:

$$F\{\Psi(\bar{r})\}\rightarrow\Psi'(\bar{k}) , \tag{41}$$

with

$$F^{-1}\{\Psi'(\bar{k})\}\rightarrow\Psi(\bar{r}) . \tag{42}$$

Since

$$F\{\nabla^2\Psi(\bar{r})\}\rightarrow-\bar{k}^2\Psi'(\bar{k}) \tag{43}$$

we have

$$F^{-1}\{-\bar{k}^2\Psi'(k)\}\rightarrow\Delta^2\Psi(\bar{r}) . \tag{44}$$

We now discuss the numerical preparation of the initial packet. We start the initial wave function with a Gaussian wave packet multiplied by the ground-state vibrational eigenfunction of the diatom in the initial arrangement, i.e.,

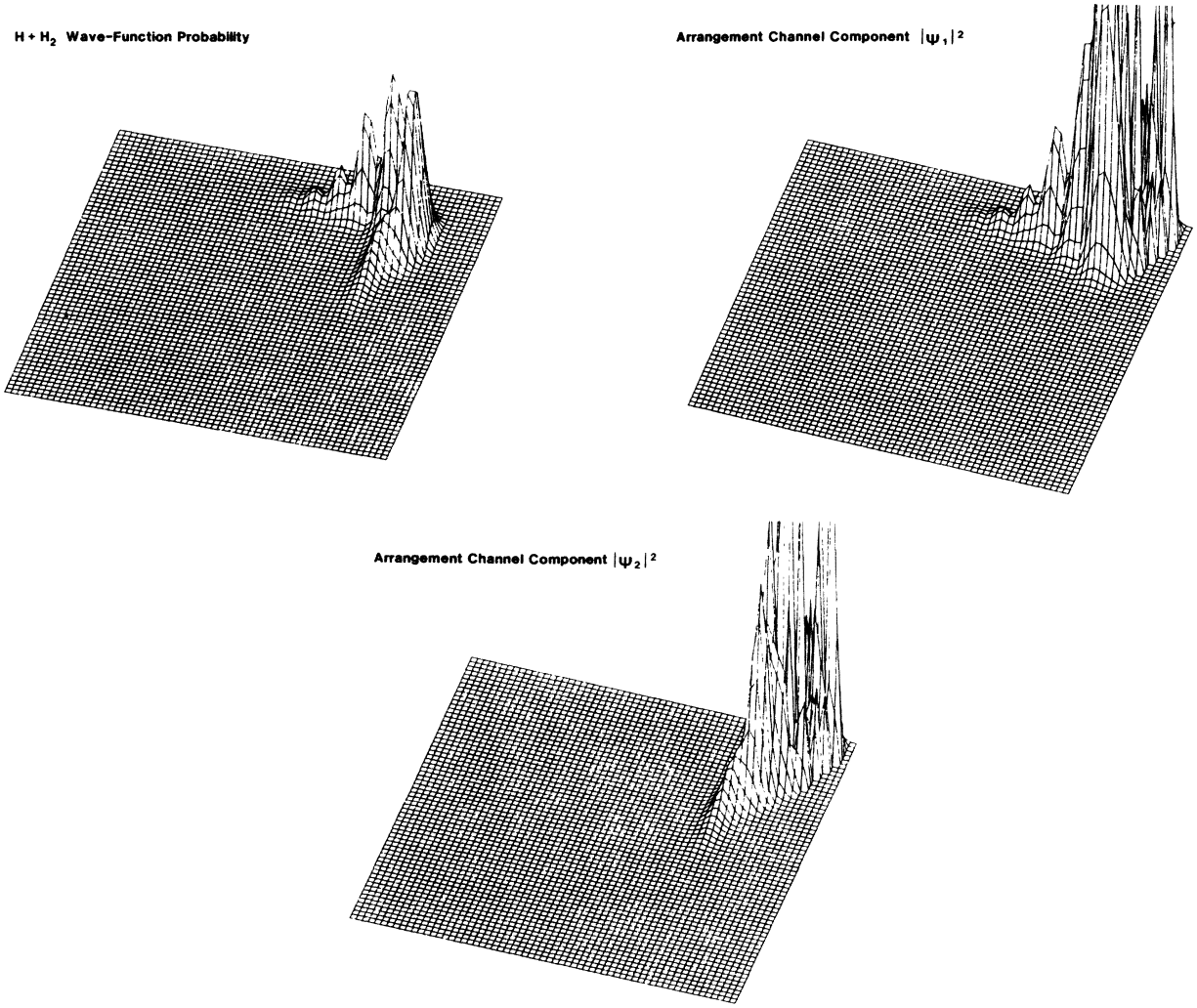

FIG. 5. Same as Fig. 4 except $t=30$.

$$\Psi_1(0)=\Phi(R)\chi(r)\ ,$$
$$\Psi_2(0)=0\ , \tag{45}$$

where

$$\Phi(R)=\frac{1}{2\pi}\int A(k)\exp(-ikR)dk$$
$$=(2\pi\delta^2)^{-1/4}\exp\{-(R-R_0)^2/4\delta^2\}\exp(ik_0R)\ , \tag{46}$$

and

$$A(k)=(8\pi\delta^2)^{1/4}\exp\{-(k-k_0)^2\delta^2\}\exp(ikR_0)\ . \tag{47}$$

The average kinetic energy of the wave packet is equal to

$$E_t(k)=\frac{\hbar^2}{2u}\left[k_0^2+\frac{1}{4\delta^2}\right]\ . \tag{48}$$

For the H_3 system,

$$\hbar^2/2u=0.003\,59\ \text{eV Å}$$

(mass scaled). The grid parameters are as follows:

$$\overline{R}_0=0.5\ \text{Å},\quad \overline{\Delta R}=0.07\ \text{Å}\ ,$$
$$\overline{r}_0=0.2\ \text{Å},\quad \overline{\Delta r}=0.06\ \text{Å}\ , \tag{49}$$
$$NR_{\max}=64,\quad Nr_{\max}=64\ .$$

The center of the wave packet is placed at $\overline{R}_c=3.0$ Å away from the origin. The system we calculated is a symmetric $H+H_2$, and the Porter-Karplus[18] potential surface is used. The time unit is 6.5793×10^{-16} sec.

III. RESULTS AND CONCLUSIONS

The symmetric stretch line is chosen to divide the potential into a reactant region and product region.[14] A reactive probability $P_r(t)$ obtained by integrating the square of the wave function in the product region is thus an average reactive probability over the energy range contained in the initial wave packet, which varies with time. Therefore if the initial wave packet is broad enough, such that its distribution in momentum space is sharply cen-

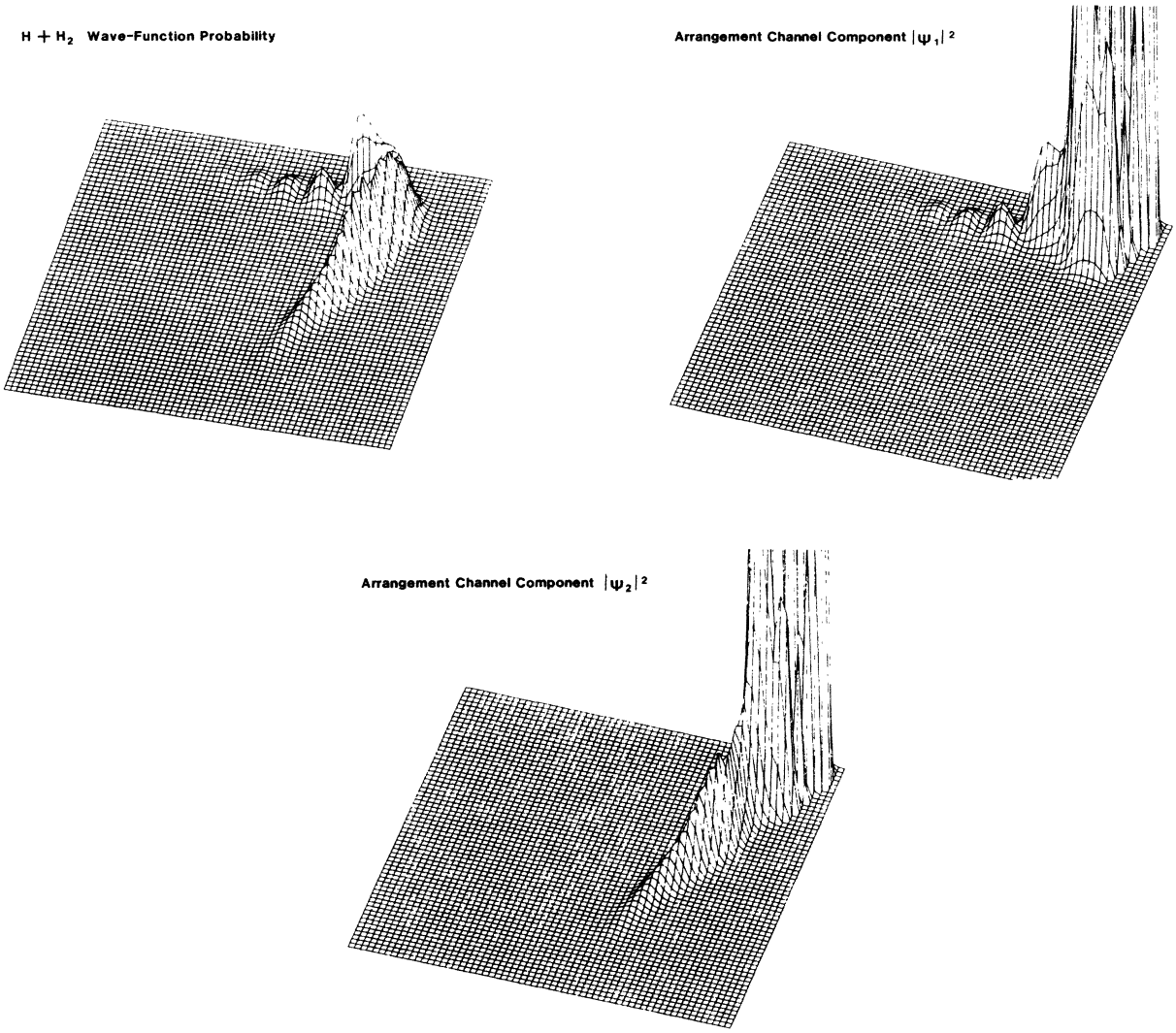

FIG. 6. Same as Fig. 4 except $t=40$.

tered around a central momentum k_0, then $P_r(t)$ will be very close to the reactive probability corresponding to single energy E_0 after enough time propagation. Different width parameters δ of the wave packet result in different average probabilities $P_r(t)$ because of the different energy distribution in initial wave packets.

Figure 1 shows the rectangular area on which our calculation is performed. The reactive probability $P_r(t)$, which depends on both time and δ, is plotted in Fig. 2, showing the effect of varying the translational shape of the initial packet. The average energies E_t at which calculations are done are 0.26, 0.38, 0.44, and 0.51 eV (all energies are below the first excited vibrational energy of H_2). Figures 3—8 depict the time evolution of the square modulus of the arrangement-channel-component states Ψ_1, Ψ_2 and total wave function Ψ. In Fig. 3 Ψ_1 propagates freely and is the same as Ψ while Ψ_2 remains zero. After moving on to Fig. 4, part of Ψ_1 has entered the interaction region and spread some into the region where the coupling potential is significant which helps create Ψ_2 in the strong-interaction region. The total wave function Ψ moves toward the product channel. As time progresses, the coupling in the interaction region becomes very strong while the reactive part of the wave function moves toward the exit channel. The amazing thing is that the giant jumps of Ψ_1 and Ψ_2 seen in the strong-interaction region are precisely out of phase and therefore cancel exactly in that region. The most important feature of these diagrams is that Ψ_1 and Ψ_2 are strictly confined to each arrangement channel except for overlapping in the strong-interaction region. In other words, Ψ_1 and Ψ_2 fully represent the total wave function away from interaction region in arrangement-channel tubes 1 and 2, respectively. This means that only the jth arrangement-channel-

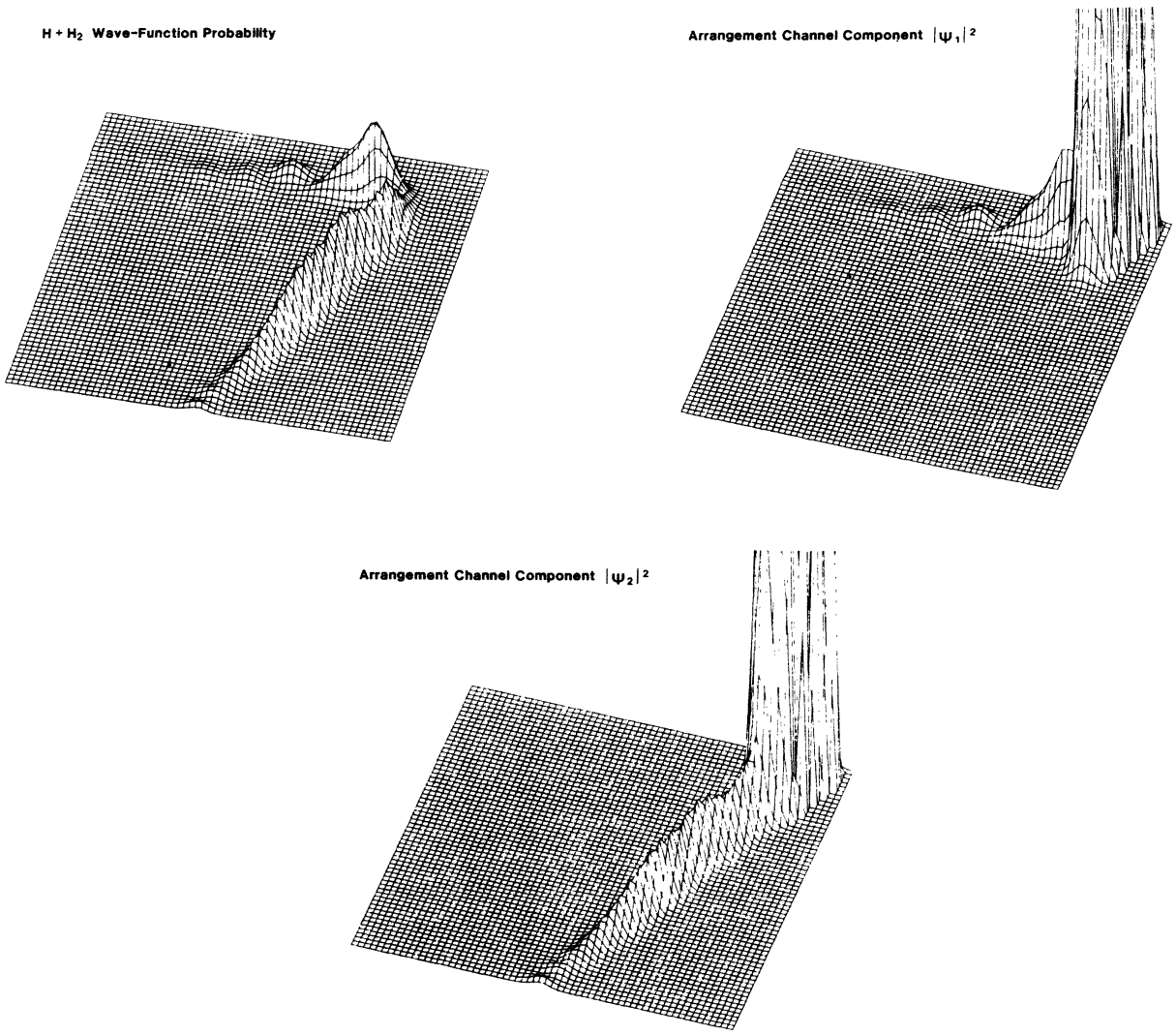

FIG. 7. Same as Fig. 4 except $t=50$.

TABLE I. Reactive probability as a function of time.[a]

Time step \ $P_r(t)$	$E_t=0.26$ eV	$E_t=0.38$ eV	$E_t=0.44$ eV	$E_t=0.51$ eV
10	0.009 397	0.016 131	0.020 218	0.025 638
20	0.069 120	0.157 572	0.213 507	0.283 208
30	0.260 548	0.534 316	0.648 010	0.747 472
40	0.533 183	0.856 157	0.889 175	0.881 797
50	0.722 099	0.964 634	0.948 537	0.889 970
60	0.796 858	0.975 284	0.952 305	0.891 811
70	0.816 096	0.935 893	0.950 779	0.890 365
80	0.819 128			

[a]The width parameter $\overline{\delta}=0.5$ Å.

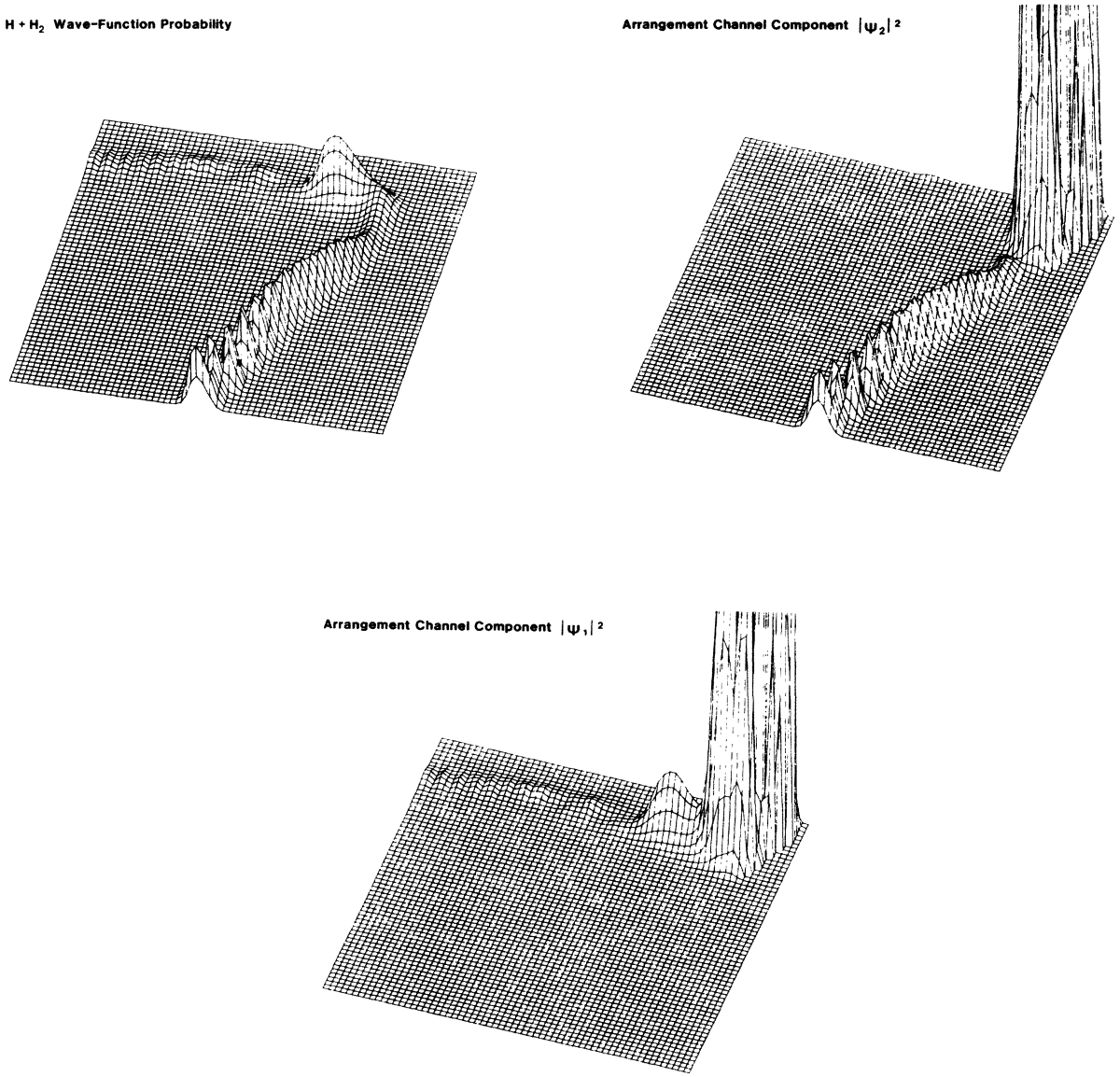

FIG. 8. Same as Fig. 4 except $t=60$.

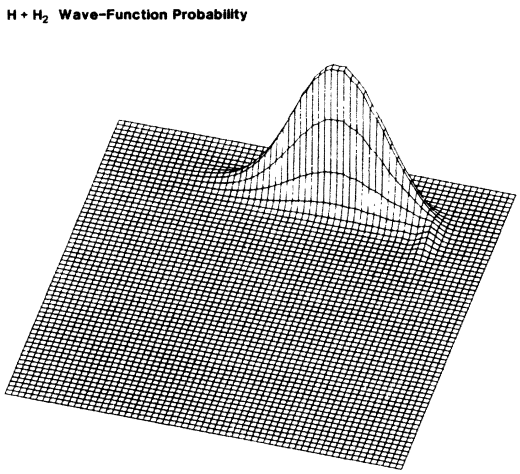

FIG. 9. Total $|\Psi|^2$ for packet with $E_t=0.38$ eV, $\delta=0.5$ Å. Time is $t=10$.

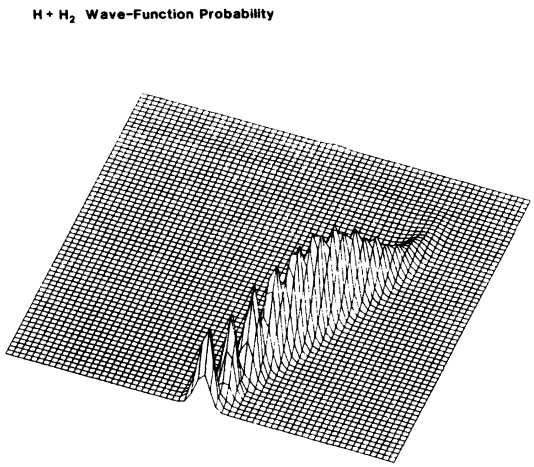

FIG. 11. Same as Fig. 9 except at $t=60$.

component state contributes to outgoing waves in that arrangement, which is a primary, fundamental feature of the ACQM equations. The question then is whether or not these jumps in Ψ_1 and Ψ_2 represent contributions of spurious solutions. Certainly spurious Ψ_1 and Ψ_2 cancel to zero and that is consistent with the behavior of these oscillations. The initial conditions used for Ψ_1 and Ψ_2 correspond to a physical solution of the ACQM equations at time $t=0$ (in the initial asymptotic region). However, numerical roundoff can introduce contributions to Ψ_1 and Ψ_2 coming from spurious solutions. The important point to note is that even though such spurious solutions may be present, they (a) cancel exactly when the full wave function is formed by adding Ψ_1 and Ψ_2 and (b) do not extend into the asymptotic regions so that Ψ_i asymptotically equals the full wave function in asymptotic channel i. Again, this reflects the fact that all scattering information in arrangement i is contained solely in arrangement-channel component Ψ_i. Because of this, the occurrence of spurious oscillations in the strong-interaction region does not create difficulties in the analysis of the scattering. Figures 9–11 are diagrams of the full wave-function probability density at the same energy $E_t=0.38$, but with $\delta=0.5$ Å. They show almost total reactivity $P_r\sim 100\%$, which is the same as the result from the stationary-state calculations. Figure 12 compares the reactive probability $P_r(t_L)$ with time-independent calculated results.[11] All the $P_r(t)$ are obtained with $\delta=0.5$ Å for the initial packet.

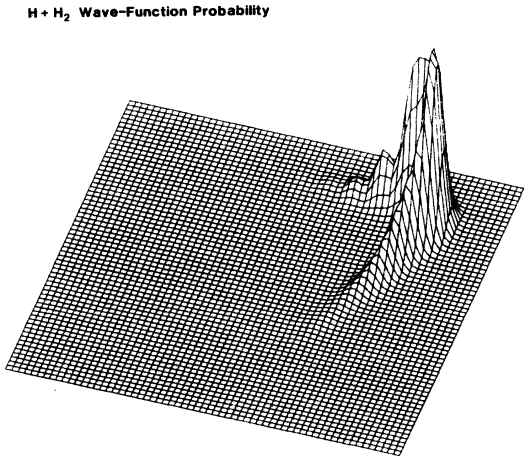

FIG. 10. Same as Fig. 9 except at $t=30$.

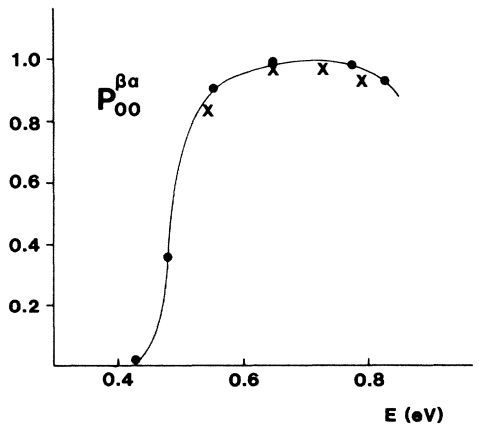

FIG. 12. Reactive probability for $V_i=0$ and $V_f=0$ as a function of total energy. Points are from D. J. Diestler, Ref. 11; crosses are our results and the solid curve is from Y. Shima, D. J. Kouri, and M. Baer, Ref. 7.

Table I presents the reactive probability $P_r(t)$ versus time of propagation at translational energies $E_t=0.26$, 0.38, 0.44, and 0.51 eV.

Finally, we note that although the solution of the time-dependent ACQM equations is of great interest from the standpoint of understanding the ACQM wave-function components Ψ_i, the computation effort in solving these equations is greater than that required to solve the time-independent ACQM or ordinary Schrödinger equations. Thus, at least the present approach does not appear promising for application in general.

ACKNOWLEDGMENTS

We wish to thank Dr. Richard Mowrey for helpful discussions of the wave-packet approach to collision problems. These calculations were carried out on the Department of Chemistry's VAX 11/780-FPS164 computing system, funded in part by grants from the National Science Foundation and Floating Point Systems. We also gratefully acknowledge support under Grant No. E-608 from the R. A. Welch Foundation.

[1]See, e.g., the overview and review (and references therein) by J. C. Light and R. E. Wyatt, in *Atom-Molecule Collision Theory: A Guide for the Experimentalist,* edited by R. B. Bernstein (Plenum, New York, 1969); and the discussion of the differential equation approach by M. Baer, in *Theory of Chemical Reaction Dynamics,* edited by M. Baer (CRC, Boca Raton, Florida, 1985).

[2]L. M. Delves, Nucl. Phys. **9**, 391 (1959); G. L. Hofacker, Naturforscher **189**, 607 (1963); R. A. Marcus, J. Chem. Phys. **45**, 4493 (1966); A. Kuppermann, J. A. Kaye, and J. P. Dwyer, Chem. Phys. Lett. **74**, 257 (1980); J. Romelt, *ibid.* **74**, 263 (1980); J. Manz and J. Romelt, J. Chem. Phys. **73**, 5040 (1980).

[3]W. H. Miller, J. Chem. Phys. **50**, 407 (1969).

[4]H. A. Askar, J. Chem. Phys. **62**, 732 (1975); A. Askar, A. S. Cakmak, and H. Rabitz, Chem. Phys. **33**, 267 (1978).

[5]See, e.g., the overview by D. J. Kouri, in *Theory of Chemical Reaction Dynamics,* edited by M. Baer (CRC, Boca Raton, Florida, 1985).

[6]M. Baer and D. J. Kouri, J. Math. Phys. **14**, 1637 (1973); Phys. Rev. A **4**, 1924 (1971); D. J. Kouri and F. S. Levin, Phys. Rev. A **10**, 1616 (1974); Nucl. Phys. A **250**, 127 (1975); W. Tobocman, Phys. Rev. C **9**, 2466 (1974).

[7]Y. Shima and M. Baer, Chem. Phys. Lett. **91**, 43 (1982); J. Phys. B **16**, 2169 (1983); Y. Shima, D. J. Kouri, and M. Baer, J. Chem. Phys. **78**, 6666 (1983); Y. Shima, D. J. Kouri, and M. Baer, Chem. Phys. Lett. **94**, 321 (1983); N. AbuSalbi, D. J. Kouri, Y. Shima, and M. Baer, J. Chem. Phys. **81**, 1813 (1984).

[8]D. J. Kouri, H. Kruger, and F. S. Levin, Phys. Rev. D **15**, 1156 (1977); J. W. Evans, D. K. Hoffman, and D. J. Kouri, J. Math. Phys. **24**, 576 (1983). Time-independent theory has been discussed, e.g., by Y. Hahn, D. J. Kouri, and F. S. Levin, Phys. Rev. C **10**, 1620 (1974); J. W. Evans, J. Math. Phys. **22**, 1672 (1981); J. W. Evans and D. K. Hoffman, *ibid.* **22**, 2858 (1981).

[9]See, e.g., F. T. Smith, Phys. Rev. A **118**, 349 (1960).

[10]K. C. Kulander, J. Chem. Phys. **69**, 5064 (1978).

[11]D. J. Diestler, J. Chem. Phys. **54**, 4547 (1971); E. A. McCullough and R. E. Wyatt, *ibid.* **54**, 3578 (1971).

[12]J. W. Evans, J. Math. Phys. **22**, 1672 (1981); J. W. Evans and D. K. Hoffman, *ibid.* **22**, 2858 (1981).

[13]L. M. Delves, Nucl. Phys. **9**, 391 (1959); **20**, 275 (1960).

[14]E. A. McCullough and R. E. Wyatt, J. Chem. Phys. **54**, 3578 (1971); A. Askar and A. S. Cakmak. *ibid.* **68**, 2794 (1978); R. Kosloff and D. Kosloff, *ibid.* **79**, 1823 (1983); R. Y. Cusson and H. W. Meldner, Phys. Rev. Lett. **42**, 694 (1979); C. Bottcher, *Advances in Atomic and Molecular Physics, (Academic, New York, 1985),* Vol. 20, pp. 246–266.

[15]H. Tal-ezer and R. Kosloff, J. Chem. Phys. **81**, 3967 (1983).

[16]D. Kosloff and R. Kosloff, J. Comput. Phys. **52**, 35 (1983); R. Kosloff and D. Kosloff, J. Chem. Phys. **79**, 1823 (1983).

[17]*Handbook of Mathematical Functions,* Natl. Bur. Stand. (U.S.) Appl. Math. Ser. No. 55, edited by M. Abramowitz and I. Stegun (U.S. GPO, Washington, D.C., 1964).

[18]R. N. Porter and M. Karplus, J. Chem. Phys. **40**, 1105 (1964).